Mixing/Segregation in Two- and Three-Dimensional Fluidized Beds: Binary Systems of Equidensity Spherical Particles

A comparison was made of the equilibrium mixing/segregation behavior of binary mixtures of different-sized, equal-density glass beads in two- and three-dimensional fluidized beds. Several empirical equations for mixing index were examined, all involving a dimensionless function of excess gas velocity. This function, which appeared to largely account for the effect of aspect ratio, was found to optimally correlate the data for both types of beds. However, a much better fit was obtained for the three-dimensional bed data, most probably because wall effects significantly retarded mixing in the two-dimensional bed.

R. W. RICE and

J. F. BRAINOVICH, JR.

Department of Chemical Engineering
Clemson University
Clemson, SC 29631

SCOPE

When an initially well-mixed bed containing solid particles of two distinct sizes and/or densities is fluidized by upflow of a gas, segregation occurs, resulting in (1) an upper portion of the bed which attains a relatively uniform composition involving both components, and (2) a lower layer which is almost exclusively composed of the less fluidizable of the two types of particles. The latter has been given the name "jetsam," denoting its tendency to sink; the other component is referred to as "flotsam." The same "equilibrium" concentration profile also occurs shortly after fluidizing an initially totally segregated bed of the same overall composition, but this case would obviously be referred to as mixing. Thus the labeling of the phenomenon as segregation or mixing depends on the initial state. The topic is of interest because of its impact on bed behavior in a number of fluid bed applications including coal combustion/gasification, ore or other dry solids separation, and waste incineration.

The solids mixing/segregation behavior of particles differing primarily in density has been studied experimentally by Rowe et al. (1972a,b), Nienow et al. (1978), Chen and Keairns (1975), and Fan and Chang (1979). Theoretical models have been proposed by Gibilaro and Rowe (1974) and Fan and Chang (1979). Most frequently it has been concluded that the main mixing mechanism involves jetsam transport in bubble wakes, while segregation involves jetsam descent by several possible means. Experiments have supported the theory that, for a given system, mixing is primarily dependent on excess gas velocity.

The experimental study undertaken here involved studying the effect of excess gas velocity, bed aspect ratio, and glass sphere size ratio on the mixing index of initially segregated beds of two radically different geometries, i.e., a conventional cylindrical three-dimensional bed and a narrow, rectangular-base, "two-dimensional" bed. Previous studies have focused on only one or the other bed type, thus one of the two main objectives of this work was to obtain a straightforward comparison of these two types of bed as regards solids mixing. A second objective was to confirm the validity of the conclusion of Nienow et al. (1978) that mixing correlations previously developed for density-differing systems do not adequately predict the behavior of size-differing, equal-density systems.

CONCLUSIONS AND SIGNIFICANCE

Equilibrium mixing index, M, vs. air velocity, U, data were obtained for binary mixtures of 128/242, 242/506, and 128/506 μm glass spheres in a 27.3 cm I.D. cylindrical bed at aspect ratios ranging from 0.28 to 0.84 and in a 28 × 2.5 × 15.2 cm rectangular-base bed. For both bed types the mixing index was found to be best correlated as a function of excess gas velocity, but the two-dimensional bed data had a greater degree of scatter and the "takeover velocity," U_{TO} (U at which $M = 0.5$), for a given two-dimensional bed was roughly twice the value for the corresponding three-dimensional bed. This fact plus photographic observation of bed behavior indicates that mixing in a two-dimensional bed is significantly hindered by:

1. The absence of out-of-line bubble coalescence
2. Lower visible bubble flow for a given excess gas velocity
3. Greater tendency toward slugging
4. Very restricted solids circulation.

Consequently, mixing/segregation data obtained in two-dimensional beds are of little quantitative value in predicting three-di-

Correspondence concerning this paper should be addressed to R. W. Rice.

mensional bed behavior.

As predicted by Nienow et al. (1978), their mixing equation for three-dimensional, density-differing systems was found to give a poor fit for the size-differing, equal-density data of this study, presumably because of the much lower segregation tendency of the latter. However, with a modified gas velocity parameter and an explicit term for size ratio, the Nienow logistic-type equation correlated the data well. An alternate correlation involving a forced analogy with axial dispersion also fit the data well except at very low M values. A weak effect of aspect ratio was observed, reflecting the role of bubbles in jetsam movement and the increase of average bubble size with bed height. In the correlations this effect was largely accounted for by the dimensionless gas velocity parameter and, specifically, by the takeover velocity value. Correlations for U_{TO} were developed for both types of beds.

The significance of this work lies in the fact that it provides a relatively simple means of estimating the effect of various operating parameters on the mixing behavior of beds consisting of two distinctly sized powders of comparable density. In particular it allows estimation of the gas velocity necessary to avoid segregation and this is important in the design of beds for a number of applications.

INTRODUCTION

Casual observation of a fluidized bed gives the impression of very rapid, efficient solids mixing, and in fact this has been experimentally confirmed in several studies (May, 1959; Kunii and Levenspiel, 1969) for beds of relatively uniform particle size and density. However, in a number of industrial applications the bed consists of solids differing sufficiently in density and/or size such that incomplete mixing (partial segregation) may occur at low gas velocities in the bubbling bed regime. One specific example is that of fluidized coal gasification (Chen and Keairns, 1975) in which coal char, agglomerated ash, and dolomite particles make up the bed. In this and other such cases both bed design and specification of operating conditions are improved if one has knowledge of (1) how bed segregation affects process efficiency, and (2) how design/operating variables affect the degree of segregation/mixing. The latter has been the subject of a number of investigations.

One of the earliest studies of segregation due to particle size (Shannon, 1959) showed that the primary variables affecting segregation are the minimum fluidization velocities of the solids and the superficial gas velocity. Numerous authors have suggested mechanisms by which particles mix (Rowe et al., 1965; Woollard and Potter, 1968; Haines et al., 1972; Merry and Davidson, 1973; Ghar et al., 1975; Werther, 1976; and Thiel and Potter, 1979) and segregate (Capes and Sutherland, 1966; Rowe et al., 1972a,b; Gibilaro and Rowe, 1974; Chen and Keairns, 1975; Rowe and Nienow, 1976; Nienow et al., 1978; Fan and Chang, 1979; and Geldart et al., 1981). There appears to be general agreement that the primary mechanism for mixing is upward transport of solids by bubble wakes, accompanied by a compensating downflow in the emulsion phase, which in large beds may establish long-range circulation patterns. Lateral mixing results from solids exchange between wakes and emulsion, physical displacement by rising bubbles, and spreading caused by erupting bubbles. Segregation is also related to bubble behavior. The drag force of the fluidizing gas in a bubbling bed at moderate gas velocities may suspend the more readily fluidized particles, i.e., flotsam, but not the denser and/or larger jetsam particles. Thus, when a bubble passes, jetsam particles have an opportunity to move downward by falling through the bubble or around it into the void left behind. In this way jetsam descends through the bed in a somewhat chaotic manner. An equilibrium condition is reached in the bed when the rate of segregation is equaled by the rate of mixing. Most observers have concluded that the time required for attainment of a new equilibrium state after an alteration in operating conditions is quite short, often less than a minute.

Using a two-dimensional bed which allowed photographic observation of the fluidization of binary mixtures, Rowe et al. (1972a) concluded that mixing/segregation is governed by the mechanisms cited above. In a similar study in a three-dimensional bed, Rowe et al. (1972b) found that segregation was much more sensitive to density ratio than to size ratio. Nienow et al., (1978), mostly using data taken for density-differing binary systems in a 3D bed, obtained the following mixing index correlation,

$$M = x/\bar{x} = (1 + e^{-Z})^{-1} \tag{1}$$

where

$$Z = \frac{U - U_{TO}}{U - U_F} e^{U/U_{TO}}. \tag{2}$$

In the equations above M is the equilibrium mixing index, x is the mass fraction of jetsam in the upper region of the bed, $\bar{x}$ is the overall bed jetsam mass fraction, U is the superficial gas velocity, U_F is the minimum fluidization velocity of the flotsam, U_{TO} is the takeover velocity defined as the U value at which $M = 0.5$, and Z is what will be called the excess gas velocity parameter. Once the Z term had been defined, the form of Eq. 1 was suggested by the sigmoidal shape of M vs. Z curves and the necessity that $M = 0.5$ at $U = U_{TO}$. The Z parameter was formulated to satisfy the observed M vs. $U - U_F$ behavior and the boundary conditions, i.e., $M = 0$ at $U \leq U_F$, $M = 1$ as $U \to \infty$. A complex equation was also presented relating U_{TO} to the ratio, U_J/U_F, of jetsam to flotsam minimum fluidization velocities; the density ratio, diameter ratio, x value, and the bed aspect ratio. While most of these studies involved relatively dense particles less than 700 μm in size and low velocities, Geldart et al., (1981) found that the Nienow equations qualitatively agreed with these observations for a density-differing system composed of much larger, e.g., 3,500 μm, low-density solids. For size-differing, equal-density systems they suggested the following proportionality,

$$M \propto \left(\frac{\bar{d}_p}{d_F}\right)^m \left[\frac{U}{U - U_F}\right]^n \tag{3}$$

where $\bar{d}_p$ and d_F are, respectively, the mass fraction-weighted mean particle diameter for the entire bed and the mean flotsam diameter, and m and n are constants that were not specified.

The work described in the present paper focused on the topic of strictly size-difference-induced segregation, in contrast to previous investigations, which were predominantly for density-differing systems. Furthermore, since the literature on this topic is split between 2D and 3D bed studies with no obvious means for interrelating the two, it was felt that it would be useful to obtain a direct comparison.

EXPERIMENTAL

Equipment and Materials

Two Plexiglas fluidized beds were used: a 3D cylindrical bed with an inside diameter of 27.3 cm, and a 2D bed with a 28 × 2.5 cm rectangular cross section. In both cases the distributor material was Porex SPFGM, a

high density porous polyethylene, 2 cm thick with an average pore diameter of 40 μm. Each distributor was sealed on its outer edges and securely fastened between the bed and lower plenum chamber with gasketed flanges. Dry, filtered compressed air was metered into the bed through a parallel network of calibrated rotameters. Manometers were connected to measure the pressure drop across both the distributor and bed. Sieve analysis was accomplished using U.S. Standard sieve plates mounted on a Cenco-Meinzer shaker. Photographic equipment used to study bubble size and frequency consisted of a Yashica FR-1 35 mm camera and a Fastax FR-17 16 mm motion picture camera.

The glass microspheres used in the study were obtained from Ferro Corporation, Cataphote Division, Jackson, Miss., and all had a particle density of 2.5 g/cm^3. Three different bead sizes were used after extensive sieving to obtain nonoverlapping, relatively narrow particle size distributions. The particle size ranges and corresponding volume average diameters were: 105–149 μm (128 μm); 210–297 μm (242 μm); and 354–590 μm (506 μm).

Preliminary Fluidization Measurements

The minimum fluidization velocity, U_{MF}, and minimum bubbling velocity, U_{MB}, for each of the three bead sizes were determined in the standard manner of monitoring bed pressure drop as superficial gas velocity, U, was increased then later decreased. Because the pressure drop vs. U curve for the largest bead size showed no sharp break characteristic of U_{MF} even after the obvious onset of bubbling, it was decided that U_{MB} would be a more reliable parameter than U_{MF} to use in later correlations. The values of these two quantities were very similar in any case. Values found for U_{MB} in the 3D bed were 1.8, 4.5 and 16.0 cm/s for the 128, 242 and 506 μm beads, respectively, independent of bed height. These are in reasonable agreement with values predicted by accepted correlations (Kunii and Levenspiel, 1969). The corresponding 2D bed U_{MB} values were 2.9, 5.9 and 16.0 cm/s. The U_{MB} values found for the smaller beads in the 2D bed were somewhat larger than expected, although some increase in U_{MB} for a 2D bed relative to a 3D bed had been anticipated based on the literature (Geldart, 1970; Cranfield and Geldart, 1974). One obvious contributing factor was the suppression of bubbling caused by the small thickness and large ratio of wall perimeter to distributor area. In both beds the distributor pressure drop was comparable to the pressure drop across the bed over most of the range studied and a very uniform lateral bubble distribution was observed.

Procedure

The experiments were conducted using the general technique employed by several previous investigators. As an example, for the 15.2 cm high 3D bed runs this involved first loading approximately 5,000 g of jetsam beads followed by 9,000 g of flotsam beads on top, giving an initially totally segregated bed with $\bar{x} = 0.356$. This $\bar{x}$ value was used in all runs. For similar 2D bed runs 580 g of jetsam were placed below 1,050 g of flotsam. All runs were conducted at ambient temperature (296–301 K) and pressure (approx. 1×10^5 N/m^2) by starting air flow at the desired initial flow rate then periodically sampling at 5–10 m intervals after rapidly "freezing" the bed in position by diverting the gas flow out of a quick-opening valve upstream of the rotameters. Sampling was done by vacuuming out roughly the top 3–4% of the bed (0.2–0.9 cm) and prompt analysis of the sample was made by sieving and weighing the flotsam and jetsam portions. The sample was then returned to the bed and the bed was refluidized. For a given gas velocity this process was repeated until two successive samples were deemed satisfactorily close (typically within 10% of the preceding x value). The average of these reproducible readings was used to calculate the equilibrium mixing index value for that velocity, then the gas velocity was changed and the process described above was repeated. This was continued until enough M values had been calculated to define the M vs. excess gas velocity curve over nearly the full range. In several cases, after a high M value had been reached, M values were also determined by successively reducing gas velocity to repeat measurements previously made in the increasing velocity mode. This was done to confirm the "equilibrium" nature of the measurement and, although very little hysteresis was found, it was noted that a measurably longer equilibration time (5–10 m vs., say, 1 m for the increasing M mode) was required. Given the absence of a density difference driving force, this relatively slow segregation is not surprising.

Figure 1 shows four cases which illustrate a representative sequence of mixing states. In the first case ($M = 0$) the bed is totally segregated; in the second ($M = 0.25$) mixing is low but uniform axially, typical of low excess gas velocity; in the third at higher gas velocity, significant mixing ($M = 0.75$) has occurred and the jetsam-rich layer at the bottom is noticeably depleted; the fourth ($M = 1$) shows idealized complete mixing. The uniform axial concentration depicted for the upper portion of a bed is what made the sampling of only a small portion of the flotsam-rich region justifiable. This uniformity was confirmed experimentally for a variety of M values in both beds. An example for a high M value (≈ 0.85) case is given by Figure 2.

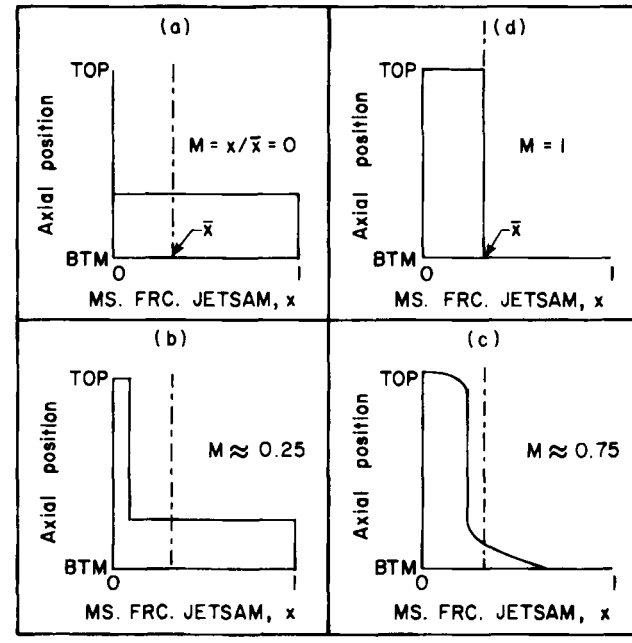

Figure 1. Idealized jetsam concentration profiles.
(a) Total segregation, $U_{EX} \leq 0$
(b) Moderate mixing, low U_{EX}
(c) Extensive mixing, moderate U_{EX}
(d) Complete mixing, very high U_{EX}

Because of the accepted importance of bubble behavior in mixing/segregation phenomena, a short study was made to determine if mixing correlated with average bubble size and/or frequency. Experimentally this involved photographing: (1) bubble eruptions for 3D beds using both 35 mm and 16 mm cameras tripod-mounted above the bed, and (2) bubbles visible in a 2D bed viewed from the side. The 35 mm still pictures were taken at a rate of 1/s for 30 s. The 16 mm moving pictures were taken at a speed of 240 fps for 6 s. In both cases numerous frames were later viewed and used to calculate average bubble diameter and point frequency.

RESULTS AND DISCUSSION

Three-Dimensional Bed Mixing Studies

In light of the multitude of variables that have been found to affect solids mixing/segregation and the time-consuming nature of the experiments, it was decided that the 3D bed portion of this study would concentrate on the effects of particle size ratio, bed aspect ratio, and gas velocity while particle density and jetsam concentration were held constant. Accordingly, seven 3D runs, involving a total of 166 data points, were made. Runs 1–3 were made using 128 μm flotsam/506 μm jetsam (size ratio, $R_d = 3.95$) at bed aspect ratios of $R_a = 0.28$, 0.56, and 0.84. Runs 4–6 involved the same three aspect ratios for 128 μm flotsam/242 μm jetsam, $R_d = 1.89$. Run 7 was made at the same aspect ratio, $R_a = 0.56$, and at nearly the same size ratio, $R_d = 2.09$, as run 5, but with both flotsam and jetsam being roughly twice as large, i.e., 242 and 506 μm, respectively.

In all of the 3D bed runs it was found that as excess gas velocity U_{EX} was increased, the mixing index initially increased very

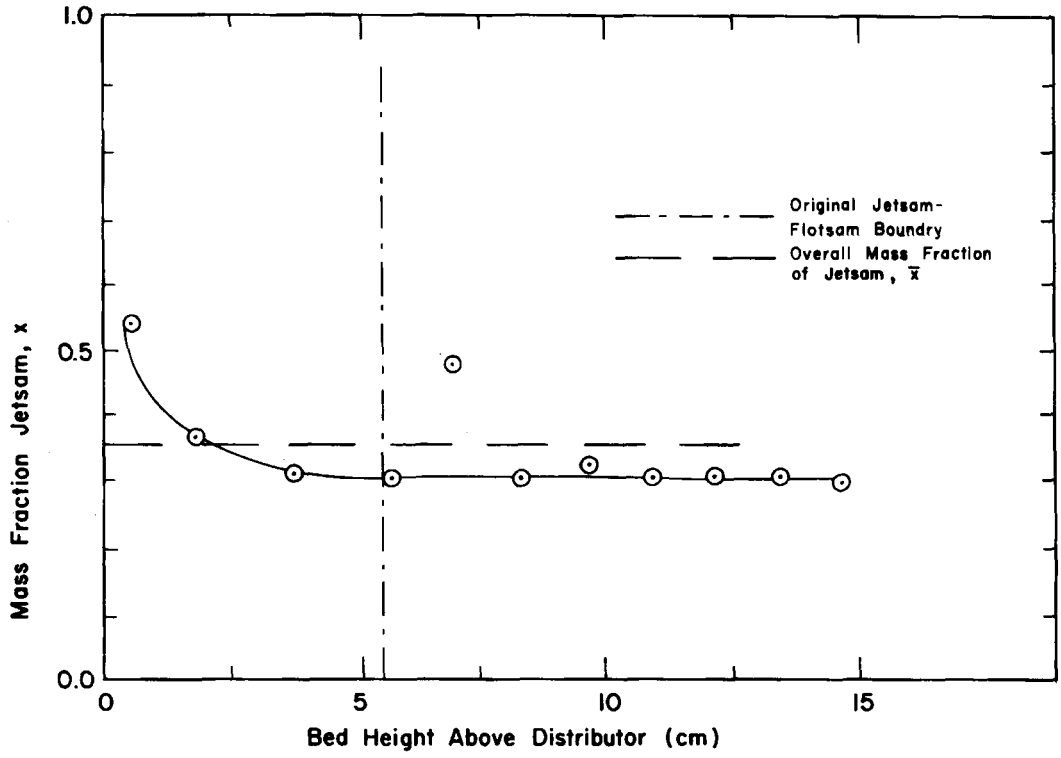

Figure 2. Experimental jetsam concentration profile.

slowly, then rose very rapidly over a narrow U_{EX} range centered about the excess takeover velocity, $U_{TO} - U_{FB}$, and finally asymptotically approached the limiting value of 1.0. Data for a typical example, run 5, are shown in Figure 3. This type of S-shaped curve was noted by previous workers (Nienow et al., 1978). Accepting that bubble behavior governs mixing, at least one reasonable hypothesis can be offered to explain the sigmoidal shape. Mixing is low at low U_{EX} because most of the bubbles in the upper flotsam-rich portion of the bed are small and rise slowly, remaining isolated until well away from the jetsam-rich underlayer. Thus, upward movement of jetsam in wakes is insufficient, in competition with segregation due to solids downflow, to maintain a high jetsam concentration in the upper region. As excess gas velocity increases, several effects occur nearly simultaneously. First, the frequency of bubble initiation in the region just above the jetsam-rich portion increases somewhat and the bubbles in this area become larger. This is predicted by Eq. 4, which is a correlation for initial spherical equivalent bubble diameter, D_o, as a function of excess gas velocity,

$$D_o \propto (U - U_{MF})^a \tag{4}$$

where a is a constant which theory (Harrison and Leung, 1961) and experimentation (Fryer and Potter, 1976) suggest lies between 0.33 and 0.4. In the nonslugging, bubbling bed regime at a given velocity, U, bubble size increases nearly linearly with distance from the distributor (Fryer and Potter, 1976) according to Eq. 5 formulated by Kato and Wen (1969),

$$D = D_o + b\left(\frac{U}{U_{MF}}\right)H' \tag{5}$$

where D is equivalent spherical bubble diameter at a height, H', and b is a constant depending linearly on particle diameter and density. In this case the nonbubbling jetsam-rich bottom layer served as a type of extended distributor. As gas velocity increases, bubble coalescence occurs nearer the flotsam/jetsam boundary, bubble rise velocity increases, and the amount of jetsam lifted in the growing wakes increases proportionately. In the vicinity of some threshold velocity, best characterized as U_{TO}, the rate of increase in wake solids transport increases markedly relative to the rate of segregation via circulation, "jetsam rain" through or around bubbles, etc. This threshold or takeover velocity would thus be expected to be a function of the properties of the jetsam as well as the flotsam, as confirmed later in this study. At velocities not much above U_{TO} the jetsam layer has become depleted, the bed is nearly homogeneous, and any further increase in U has little effect.

When the mixing index correlation, Eqs. 1 and 2, was applied to the experimental data of Figure 3, the fit was rather poor; most notably at higher excess air velocities where the Nienow correlation appreciably underpredicted the extent of mixing. This trend was not limited to Run 5, but held for all runs at high U (and Z), as shown in Figure 4. The dotted curve in Figure 3 represents the first of two correlations developed during this study for predicting the variation of M with U. The second (Z*) correlation, whose curve is also shown, will be discussed later. The first correlation developed here was an attempt to retain the Z parameter used by Nienow et al. (1978), but to improve the fit in the region of high M value. This is represented by Eq. 6,

$$M = 0.5 + 0.5\text{erf}(Z) \tag{6}$$

where *erf* is the error function defined by,

$$\text{erf}(Z) = \frac{2}{\sqrt{\pi}}\int_0^Z e^{-y^2}dy \tag{7}$$

with y being a dummy variable of integration.

The two constants in Eq. 6 were dictated by the boundary conditions, i.e., $M \to 0$ as $U \to U_{FB}$ ($Z \to -\infty$), $M = 0.5$ at $U = U_{TO}$ ($Z = 0$), and $M \to 1$ as U and $Z \to \infty$. The selection of this equation was prompted by the perhaps purely coincidential similarity of the M vs. Z data to that observed for dimensionless outlet tracer concentration vs. dimensionless time for a small

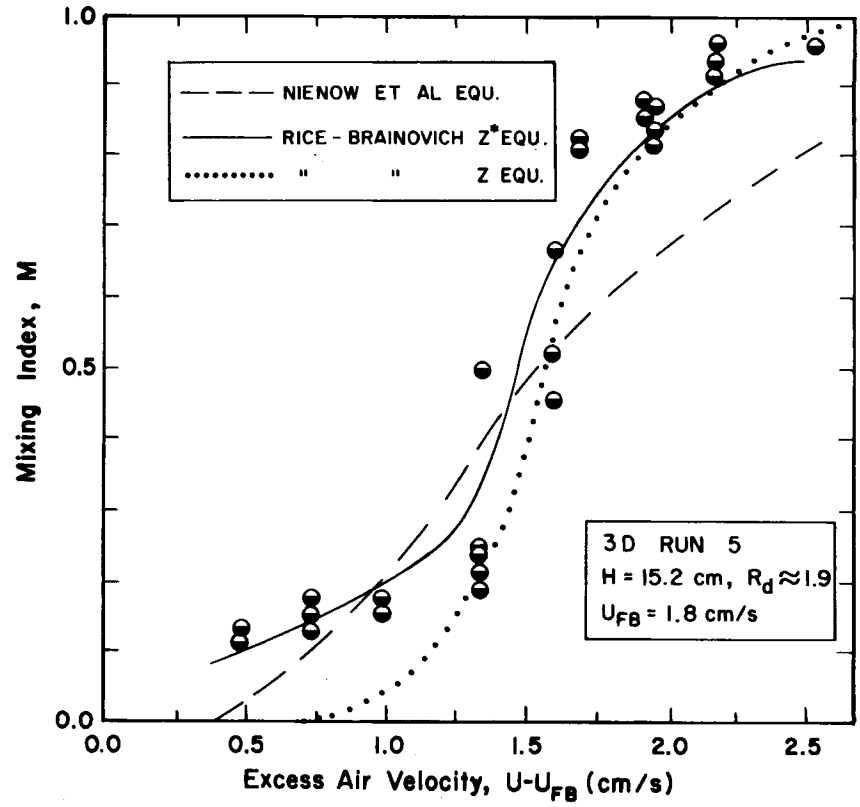

Figure 3. Mixing index as a function of excess air velocity for run 5.

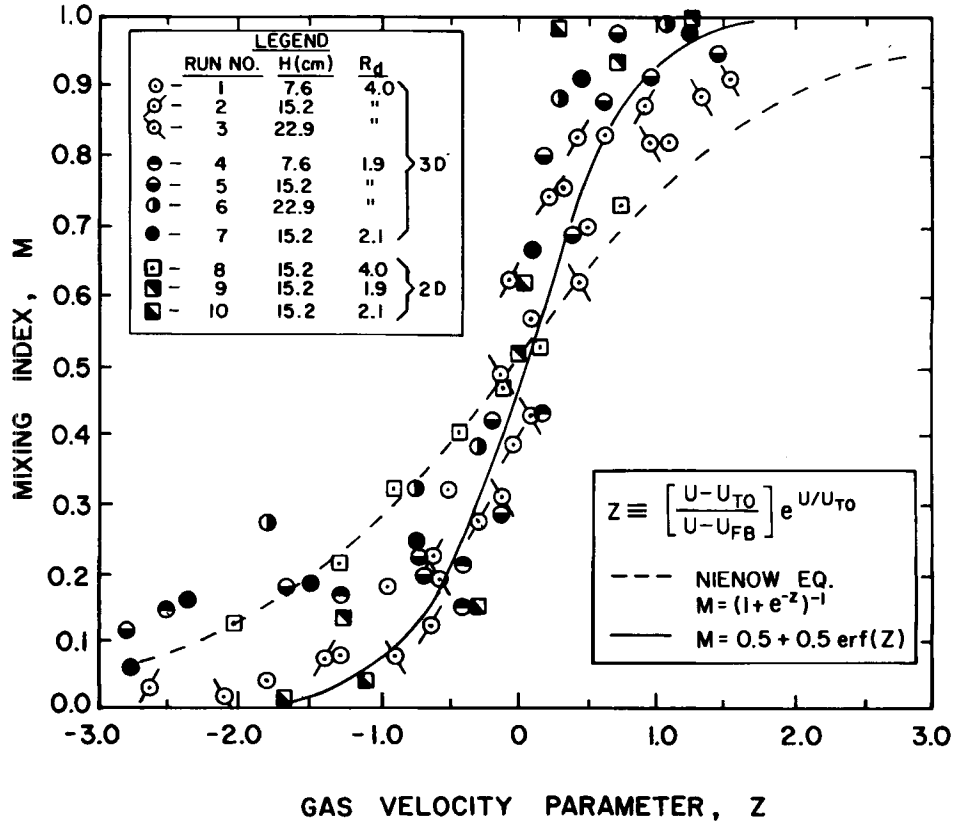

Figure 4. Overall plot of mixing index vs. Nienow reduced velocity parameter, *Z*.

degree of axial dispersion (with some bypassing) in a tubular reactor for a step function tracer input (Hill, 1977). Figure 4 shows that Eq. 6 gave a much improved fit. The variance, σ^2, for the predicted vs. measured M values gives a quantitative index of fit, with zero as perfect, and for this correlation a variance of 0.0130 was calculated for the seven 3D runs taken together. For the Nienow equation the corresponding value was 0.0225, thus the new correlation gave a 42% reduction in variance or, equivalently, a 24% reduction is standard deviation, *SDM*, from 0.150 to 0.114. This advantage was only slightly lowered when the 2D data were also included.

Although Eq. 6 was an advance over available correlations for this type of system, it failed to predict well at low values of U_{EX}; thus a still better correlation was sought. After evaluating numerous equations relating M and Z, it was decided that significant additional improvement required modifying the Nienow Z parameter. Various expressions for a new reduced gas velocity parameter, Z', were tested in the Nienow equation and several modifications of it. For example, with α, β, and γ as chosen constants, the general correlation represented by Eqs. 8 and 9 was tried over a range of α, β, γ values.

$$M = 2^{\gamma-1}(1 + e^{-Z'})^{-\gamma} \tag{8}$$

$$Z' = \left[\frac{U - U_{TO}}{U - U_{FB}}\right]^{\alpha} e^{\beta(U/U_{TO})} \tag{9}$$

The equations found to minimize the variance while still satisfying the boundary conditions were:

$$M = (1 + e^{-Z'})^{-1} \tag{10}$$

$$Z' = \pm\sqrt{\frac{U - U_{TO}}{U - U_{FB}}}\, e^{U/U_{TO}} \tag{11}$$

where the $\pm$ sign implies a negative Z' value for $U < U_{TO}$ and a positive Z' value for $U > U_{TO}$. This is merely the Nienow equation with the Z term altered as shown in Eq. 11. This gave a variance of 0.0104 for the overall 3D bed data, a 20% improvement over Eq. 6 and 54% over the Nienow correlation. A modest (11%) additional reduction in variance, to a value of 0.0092, was achieved by multiplying the Z' term above by the square root of a particle diameter ratio factor, f_s, defined as follows,

$$f_s = \frac{3}{R_d} \text{ for } U > U_{TO};\ f_s = \frac{R_d}{3} \text{ for } U < U_{TO} \tag{12}$$

to yield,

$$Z^* = Z' \cdot \sqrt{f_s} \tag{13}$$

This parameter was used in place of Z' in Eq. 10 to predict the M vs. Z^* curve for the overall data set shown in Figure 5 and for the three runs at different R_d values, but constant aspect ratio, shown in Figure 6.

Compared to the curve for Eq. 6 in Figure 4, the Z^* correlation curve of Figure 5 fits the low velocity data appreciably better and does nearly as well at high U values. A fair degree of scatter is seemingly inherent in such experimental mixing data, as illustrated by similar figures in papers by Rowe and Nienow (1976) and Nienow and Rowe (1978). One reason for this is the extreme sensitivity of M to U (and thus to Z^* or Z) in the region around U_{TO}, which makes slight variations in the measurement of U cause

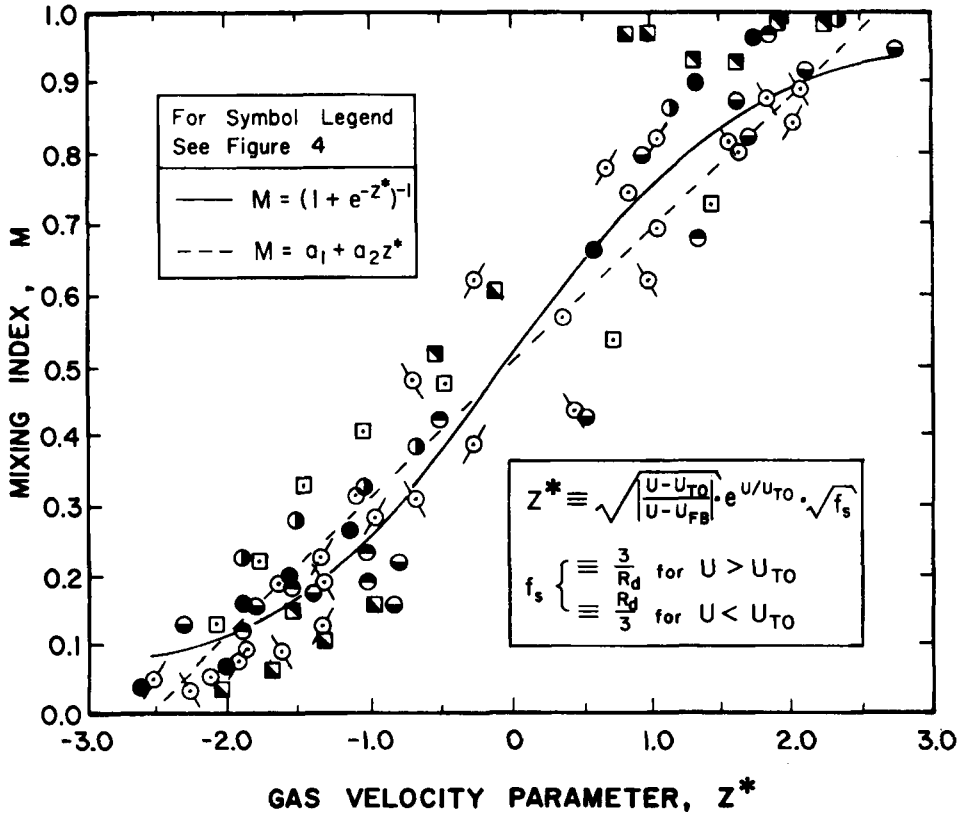

Figure 5. Overall plot for the Z^* mixing correlation.
$Z^* < 0$ for $U < U_{TO}$
$Z^* > 0$ for $U > U_{TO}$

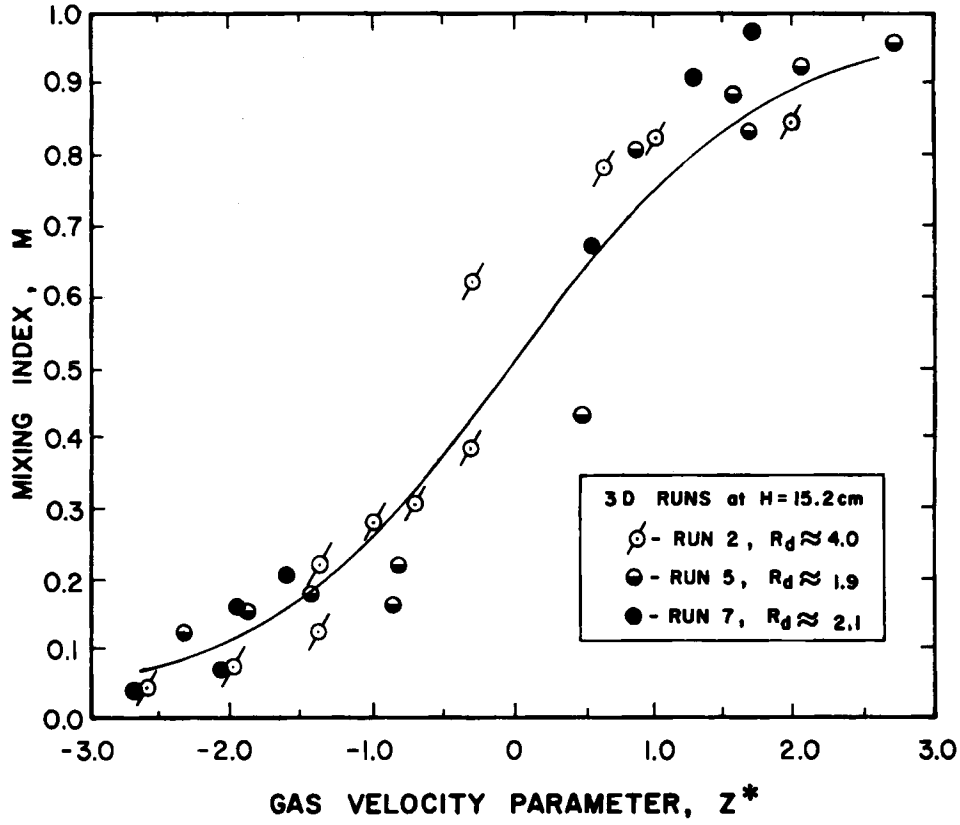

Figure 6. Mixing index vs. Z^* air velocity parameter for the 3D runs at $R_d = 0.56$.

large variations in M value. Considering this possible experimental error and the diversity in bed geometry, etc., involved in the 10 runs, it is believed that the Z^* correlation is very close to optimal, yet is relatively simple. As a last comment on Figure 5, it should be pointed out that, out of curiosity, a least-squares line given by $M = 0.194Z^* + 0.49$ was fitted to the entire set of 3D and 2D data as shown. This equation gave a variance only slightly higher than that of Eq. 10, but is not recommended because it does not satisfy the boundary conditions.

The success of this or any similar mixing correlation for prediction purposes depends critically on having a good value for U_{TO}. Given the still limited theoretical and experimental data bases for mixing phenomena, it is clearly advisable to measure U_{TO} experimentally in a pilot-scale fluid bed. Nevertheless, the data from the seven 3D runs of this study did provide the basis for formulating a predictive equation for U_{TO}. Nienow et al. (1978) developed a complex correlation for U_{TO} as a function of six variables and containing eight constants, but specified that their equation was not applicable to equidensity systems such as the ones in this study. Indeed, their correlation overpredicts U_{TO} for the cases considered here by factors ranging from 2 to 5, confirming the expectation that mixing of equidensity systems is considerably easier than for density-differing systems of comparable size. Table 1 shows data used to obtain the equidensity 3D bed U_{TO} correlation, presented below as Eq. 14, which was found to give the best predictions of various forms tried.

$$U_{TO,3D} = (U_{FB}U_{JB})^{0.5}(2R_a)^{-0.2} \tag{14}$$

Considering the simplicity of the equation, the fact that the predicted U_{TO} value was within ± 15% of the measured value for all but run 6 is encouraging. This empirical equation is applicable only for equal-density 3D systems and was obtained using data

Table 1. Summarized Data and Results for the Takeover Velocity Correlations

Run No.	Bed Type	Bed Height H cm	Ratio R_d	U_{FB} cm/s	U_{JB} cm/s	U_{TO}/U_{FB}	U_{TO}/U_{JB}	Measured U_{TO} cm/s	Predicted U_{TO} (Eq. 14) cm/s	% Error in U_{TO} Pred.
1	3D	7.6	3.95	1.8	16.0	3.00	0.34	5.4	6.0	+12
4	3D	7.6	1.89	1.8	4.5	1.89	0.76	3.4	3.2	− 6
3	3D	22.9	3.95	1.8	16.0	2.44	0.28	4.4	4.8	+10
6	3D	22.9	1.89	1.8	4.5	1.94	0.78	3.5	2.6	−27
2	3D	15.2	3.95	1.8	16.0	2.72	0.31	4.9	5.2	+ 7
5	3D	15.2	1.89	1.8	4.5	1.83	0.73	3.3	2.8	−15
7	3D	15.2	2.09	4.5	16.0	1.78	0.50	8.0	8.3	+ 4
8	2D	15.2	3.95	2.9	16.0	3.83	0.69	11.1	(Eq. 15) 10.8	− 3
9	2D	15.2	1.89	2.9	5.9	2.07	1.02	6.0	5.8	− 3
10	2D	15.2	2.09	5.9	16.0	2.51	0.92	14.8	16.8	−13

for only one particle density and $\bar{x}$ value. However, based on Nienow's results, $\bar{x}$ has a very small effect on U_{TO} and the effect of particle density is more or less implicit in the $U_{FB} \cdot U_{JB}$ term. The low value of the exponent for the aspect ratio term reflects the relatively weak dependence of U_{TO} on R_a found here. Previous investigators, e.g., Nienow et al. (1978), have commented that mixing improves slowly with increasing bed height, possibly because of the increase in bubble coalescence. For runs 1–3 U_{TO} decreased with increasing R_a, but for runs 4–6 U_{TO} was essentially constant within experimental error, thus aspect ratio becomes more important as R_d increases. For the M vs. Z^* correlation, no explicit term for R_a was included because, as Figure 7 illustrates, the effect was apparently well accounted for by the U_{TO} value. The curves shown in this figure are those predicted by the Z^* correlation.

Two-Dimensional Bed Mixing Studies

It was felt that a good comparison of 2D and 3D bed mixing behavior could be obtained by making 2D bed runs using the same middle range bed height, 15.2 cm, the same $\bar{x}$ value, and the same bead combinations as in the 3D runs. Thus three 2D bed runs, labeled 8, 9, and 10, were made, involving a total of 51 measurements, for later comparison with the corresponding 3D bed runs 2, 5, and 7, respectively.

From Figure 5 it can be seen that, although the data from the three 2D bed runs follows a pattern qualitatively similar to that for the 3D bed runs, the 2D bed data consistently fell on the outer portion of the "envelope." This illustrates one general finding of this study, namely that although the same correlation was found to give the best fit (of the various ones tried) for both types of beds, the fit for the 2D bed runs was not nearly as good as for the 3D bed runs. Figure 8 summarizes the 2D bed data with each point plotted representing the average of roughly three M values at a given gas velocity. The Z^* correlation curve clearly maps the general trend in the data, but the variance here, $\sigma^2 = 0.0194$, is slightly more than twice the value, 0.0092, for the 3D bed data. Runs 9 and 10, both with R_d approximately equal to 2, gave sigmoidal-shaped M vs. U_{EX} plots somewhat like the 3D runs, but in run 10 the onset of measurable mixing was at an abnormally high velocity and M then increased unusually rapidly. On the other hand, in run 8 with $R_d = 4$ appreciable mixing occurred at a lower velocity than expected and, unlike any other runs, increased in a linear fashion with increasing U_{EX}.

Table 1 provides information which makes some of these abnormalities more understandable. First, the takeover velocities for the 2D runs were approximately twice the U_{TO} values for the corresponding 3D runs, and for runs 8 and 9 U_{TO} was essentially equal to the U_{JB} value, whereas for the corresponding 3D runs it was roughly $1/2$ to $3/4$ of U_{JB}. This indicates that mixing in the 2D bed was significantly retarded in relative terms and did not become appreciable until the entire bed was in a fluid state. The reason for this difference is almost certainly that the thin layer geometry of the 2D bed made wall effects dominant, greatly restricting bubble growth and consequently impeding upward jetsam transport in wakes. Geldart (1970) in comparing bubble behavior in 2D and 3D beds found that under the same fluidization conditions the average bubble diameter for a 3D bed is larger than that for a 2D bed. The difference was attributed to the fact that in a 2D bed out-of-line bubble coalescence is impossible in the direction normal to the flat side. Furthermore, Geldart observed that a lower percentage of the excess gas volume was detectable as visible bubbles in a 2D bed compared to a 3D bed.

The odd behavior of run 8 is also explainable along these lines. From Table 1 it should be noted that U_{TO} for run 8 was much higher, roughly 4 U_{FB}, than in any other runs. This is consistent with the fact that the bed was observed to begin visible slugging before M values above 0.5 could be reached. It is reasonable to assume that this occurred here and not in runs 9 or 10 because in run

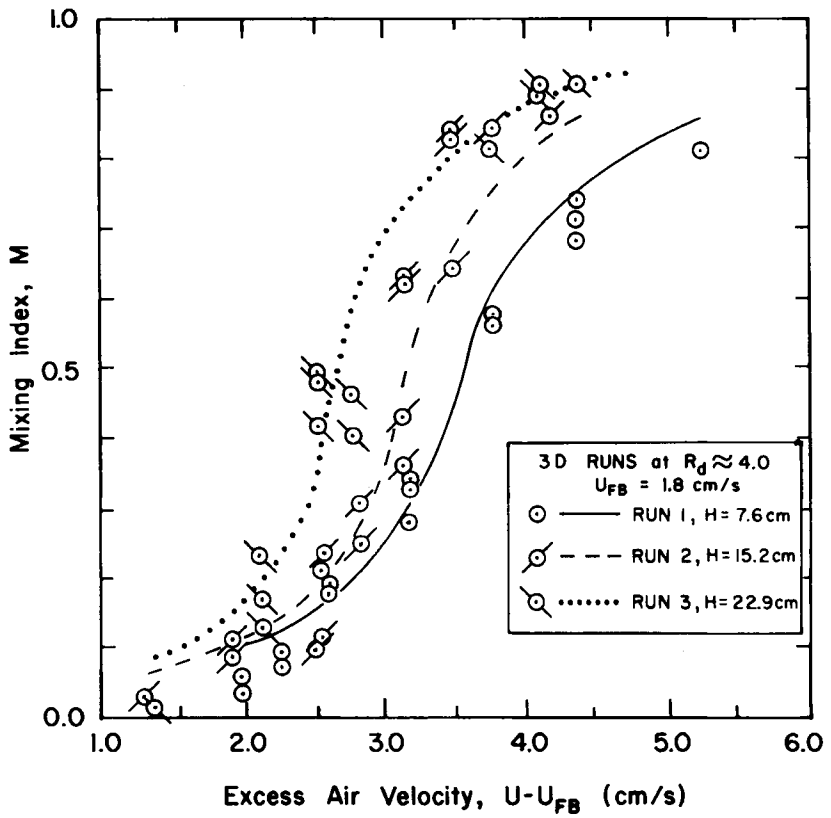

Figure 7. The effect of aspect ratio on mixing for constant size ratio.

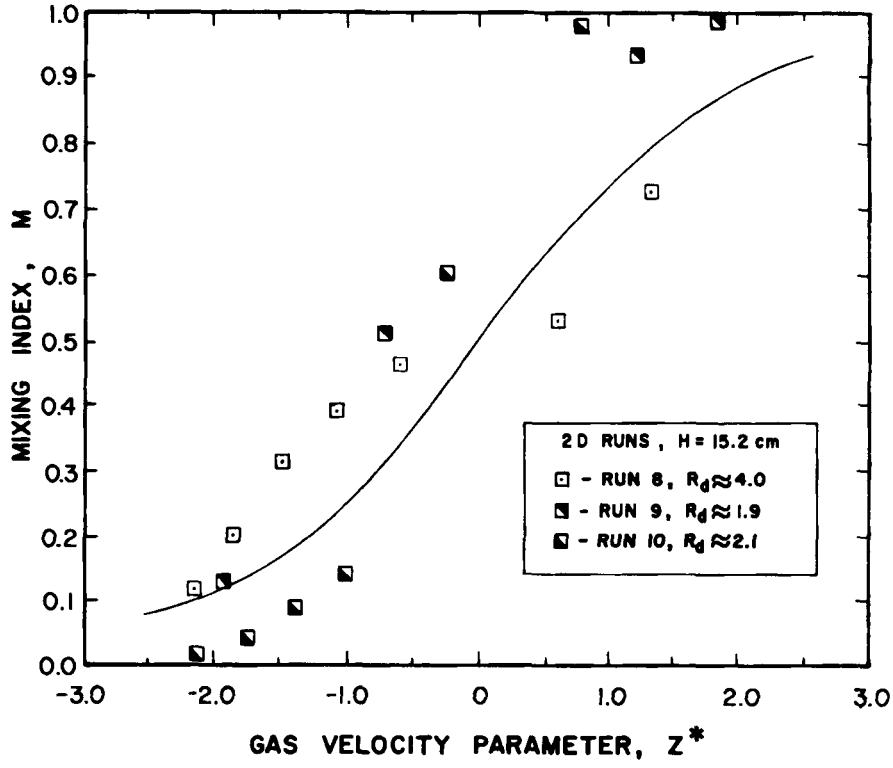

Figure 8. Two-dimensional bed mixing data.

8 with R_d = 4, the U_{JB}/U_{FB} ratio was very large (5.5) compared to that for the other 2D runs (2.0 and 2.7); thus by the time that a bubble velocity sufficient to "lift" the jetsam had been reached, the bed was on the verge of slugging. In this state jetsam could not be efficiently mixed with the overlying flotsam-rich layer because the entire cross section of the bed was periodically occupied by a single bubble. The rapid rise of M noted for all other runs in the vicinity of U_{TO} and attributed to sudden widespread bubble coalescence was absent in run 8 because complete coalescence, i.e., slugging, began a bit below U_{TO} and further increases in U_{EX} only gradually increased the extent of mixing. An equivalent circular diameter, D_{eq}, of 4.7 cm was calculated for the rectangular cross section of the 2D bed using the fluid dynamics relation that states that D_{eq} is four times the hydraulic radius. For all of the 2D runs this gave R_a = 3.26. Using this value, the predictive equation for U_{TO} based on 3D data predicted 2D bed U_{TO} values roughly half those measured. A separate correlation, Eq. 15, gave a good fit to the 2D data as shown in Table 1,

$$U_{TO,2D} = (U_{FB}U_{JB})^{0.62}, \qquad (15)$$

but since only a single value of R_a was studied, its general applicability is unknown.

Photographic Study of Bubble Characteristics

A short supplemental study was made to measure bubble size and frequency in an attempt to relate such measurements to the mixing data. Both 16 mm moving and 35 mm still pictures were taken of bubble eruptions at the top of 3D beds, and of entire bubbles viewed from the large side of 2D beds. Bubble size and point frequency were then determined from the film using the procedure and equations recommended by Geldart (1970).

Four cases were examined, cases 1 and 2 using the motion picture camera and cases 3 and 4 using the still camera. Measured values of corrected average bubble diameter and point frequency at the bed surface for the four cases are given in Table 2. Bubble diameter values shown are the equivalent spherical values.

The results of cases 1 and 2 provide an informative direct comparison of the effectiveness of bubbles to induce mixing in 2D and 3D beds of the same flotsam/jetsam loading (242/506 μm) and height (15.2 cm). Note that, consistent with a higher excess velocity (6.9 vs. 2.1 cm/s), the bubble point frequency for the 2D bed of case 2 was over twice that for the 3D bed and the average bubble diameter was 35% larger; yet the measured M value for the 2D bed case was only half of that for the corresponding 3D bed case. This is consistent with the general observation made earlier that

Table 2. Bubble Frequency and Size Data from Photographic Measurements

Film Case No.	Run No.	Bed Type	Excess Air Velocity U_{EX} cm/s	Bubble Freq. f s^{-1}	Measured Avg. Bubble Dia. d_B cm	Measured Mixing Index M	Predicted* Mixing Index
1	7	3D	2.1	2.2	1.7	0.20	0.18
2	10	2D	6.9	4.8	2.3	0.10	0.25
3	1	3D	3.1	—	1.3	0.32	0.24
4	2	3D	3.1	—	2.4	0.42	0.44

Using the Z correlation

wall effects greatly reduce the jetsam-lifting ability of bubbles in a 2D bed relative to a 3D bed. Cases 3 and 4 provide a comparison of bubble size and its effect on mixing index for two 3D beds with the same loading (128/506 μm) at the same excess velocity but using different heights (7.6 and 15.2 cm). Table 2 shows that, as expected, average bubble size increased nearly linearly with bed height and the measured M value for the higher bed was 31% larger. The latter is in line with the conjecture that at a given U_{EX} value mixing improves with increasing 3D bed aspect ratio due to a greater jetsam transport ability for the larger bubbles' wakes in the uppermost region. The standard two-phase theory of fluidization predicts that total bubble volume in the bed is directly proportional to excess gas velocity and thus, at a given U_{EX} increased bubble size due to coalescence is offset by a corresponding decrease in bubble frequency (Werther, 1974; Chavarie and Grace, 1975). Viewed this way, a decrease in U_{TO} with increasing aspect ratio would seem to say that bubble size has a greater effect on mixing than bubble frequency, if these are considered separately. This may be due to shape factor and/or wake fraction changes that accompany bubble growth (Naimer et al., 1982).

ACKNOWLEDGMENT

The authors gratefully acknowledge the assistance of John McLaughlin in constructing the apparatus, and of Ronald Kopczyk in performing the photographic work.

NOTATION

a = exponent for excess gas velocity, Eq. 4
a_1 = intercept value at $Z^* = 0$ in linear correlation for M, Fig. 5
a_2 = slope value in M vs. Z^* linear correlation, Fig. 5
b = slope of linear equation (Eq. 5) relating bubble diameter to bed height
d_B = average corrected spherical bubble eruption diameter, cm
d_F = mean flotsam diameter in Eq. 3
d_p = mass fraction-weighted mean particle diameter for the entire bed, Eq. 3
D = equivalent spherical bubble diameter at height H', Eq. 5
D_{eq} = equivalent circular diameter for the 2D bed, cm
D_o = initial equivalent spherical bubble diameter at $H' = 0$, Eqs. 4 and 5
f = average point frequency for bubble eruption, s^{-1}
f_s = particle size ratio correction factor defined in Eq. 12
H = bed height, cm
H' = height above the distributor, Eq. 5
m = constant exponent of particle diameter ratio, Eq. 3
M = mixing index, $x/\bar{x}$
n = constant exponent of gas velocity ratio, Eq. 3
R_a = bed aspect ratio, height/diameter
R_d = jetsam to flotsam average particle diameter ratio
SDM = standard deviation in the predicted vs. measured M values
U = superficial gas velocity, cm/s
U_{EX} = excess gas velocity, $U - U_{FB}$, cm/s
U_F = minimum fluidization velocity of the flotsam
U_{FB} = minimum bubbling velocity of the flotsam, cm/s
U_J = minimum fluidization velocity of the jetsam
U_{JB} = minimum bubbling velocity of the jetsam, cm/s
U_{TO} = takeover velocity, U value at which $M = 0.5$
x = mass fraction jetsam in the upper region of the bed
$\bar{x}$ = overall mass fraction jetsam in the bed
y = dummy variable of integration, Eq. 7
Z = dimensionless gas velocity parameter defined by Eq. 2
Z' = dimensionless gas velocity parameter defined by Eq. 11
Z^* = dimensionless gas velocity parameter defined by Eq. 13

Greek Letters

α = constant exponent of the excess gas velocity ratio term in Eq. 9
β = constant in Eq. 9
γ = constant in Eq. 8
σ^2 = variance in the predicted vs. measured M values

LITERATURE CITED

Capes, A. E., and J. P. Sutherland, "Ore Separation in a Packed-Fluidized Bed," *Ind. Eng. Chem. Proc. Des. Dev.*, **5**, 330 (1966).
Chavarie, C., and J. R. Grace, "Performance Analysis of a Fluidized-Bed Reactor. I: Visible Flow Behavior," *Ind. Eng. Chem. Fund.*, **14** (2), 75 (1975).
Chen, J. L.-P., and D. L. Keairns, "Particle Segregation in a Fluidized Bed," *Can. J. Chem. Eng.*, **53**, 395 (1975).
Cranfield, R. R., and D. Geldart, "Large Particle Fluidization," *Chem. Eng. Sci.*, **29**, 935 (1974).
Fan, L. T., and Y. Chang, "Mixing of Large Particles in Two-Dimensional Gas Fluidized Beds," *Can. J. Chem. Eng.*, **57**, 88 (1979).
Fryer, C., and O. E. Potter, "Experimental Investigation of Models for Fluidized Bed Catalytic Reactors," *AICHE J.*, **22**, 38 (1976).
Geldart, D., "The Size and Frequency of Bubbles in Two- and Three-Dimensional Gas-Fluidized Beds," *Powder Technol.*, **4**, 41, (1970).
Geldart, D., et al., "Segregation in Beds of Large Particles at High Velocities," *Powder Technol.*, **30**, 195 (1981).
Ghar, R. N., A. Kumar, and P. S. Gupta, "Blending of Solid Particles in a Fluidized Bed," *Ind. J. Technol.*, **13**, 215 (1975).
Gibilaro, L. G., and P. N. Rowe, "A Model for a Segregating Gas Fluidized Bed," *Chem. Eng. Sci.*, **29**, 1,403 (1974).
Haines, A. K., R. P. King, and E. T. Woodburn, "The Interrelationship between Bubble Motion and Solids Mixing in a Gas Fluidized Bed," *AICHE J.*, 18, 591 (1972).
Harrison, D., and L. S. Leung, "Bubble Formation at an Orifice in a Fluidized Bed," *Trans. Inst. Chem. Engrs.*, **39**, 409 (1961).
Hill, C. G., Jr., *An Introduction to Chemical Engineering Kinetics and Reactor Design*, Wiley, New York, 399 (1977).
Kato, K., and C. Y. Wen, "Bubble Assemblage Model for Fluidized-Bed Catalytic Reactors," *Chem. Eng. Sci.*, **24**, 1,351 (1969).
Kunii, D., and O. Levenspiel, *Fluidization Engineering*, Wiley, New York, (1969).
May, W. G., "Fluidized-Bed Reactor Studies," *Chem. Eng. Prog.*, **55**, 49 (1959).
Merry, J. M. D., and J. F. Davidson, "Gulf Stream Circulation in Shallow Fluidized Beds," *Trans. Inst. Chem. Engrs.*, **51**, 361 (1973).
Naimer, N. S., T. Chiba, and A. W. Nienow, "Parameter Estimation for a Solids Mixing/Segregation Model for Gas Fluidized Beds," *Chem. Eng., Sci.*, **37**, 1,047 (1982).
Nienow, A. W., P. N. Rowe, and L. Y.-L. Cheung, "A Quantitative Analysis of the Mixing of Two Segregating Powders of Different Density in a Gas Fluidized Bed," *Powder Technol.*, **20**, 89 (1978).
Rowe, P. N., et al., "The Mechanisms of Solids Mixing in Fluidized Beds," *Trans. Inst. Chem. Engrs.*, **43**, T271 (1965).
Rowe, P. N., A. W. Nienow, and A. J. Agbim, "The Mechanisms by which Particles Segregate in Gas Fluidized Beds—Binary Systems of Near-Spherical Particles," *Trans. Inst. Chem. Engrs.*, **50**, 310 (1972a).
———, "A Preliminary Quantitative Study of Particle Segregation in Gas Fluidized Beds—Binary System of Near-Spherical Particles," *Trans. Inst. Chem. Engrs.*, *50*, 324 (1972b).
Rowe, P. N., and A. W. Nienow, "Particle Mixing and Segregation in Gas Fluidized Beds, A Review," *Powder Technol.*, **15**, 141 (1976).
Shannon, P. T., "Fluid Dynamics of Gas Fluidized Batch System," Ph.D. Thesis, Illinois Institute of Technology (1959).
Thiel, W. J., and O. E. Potter, "The Mixing of Solids in Slugging Gas Fluidized Beds," *AICHE J.*, **24**, 561 (1978).
Werther, J., "Bubbles in Gas Fluidized Beds." *Trans. Inst. Chem. Engrs.*, **52**, 149 (1974).
———, "Convective Solids Transport in Large-Diameter Gas Fluidized Beds," *Powder Technol.*, **15**, 155 (1976).
Woollard, I. N. M., and O. E. Potter, "Solids Mixing in Fluidized Beds," *AICHE J.*, **14**, 338 (1968).

Manuscript received Sept. 4, 1984, and revision received Jan. 9, 1985.